

THERMODYNAMIC AND MESOSCOPIC MODELING OF TUMBLING NEMATICS, OF SHEAR-THICKENING FLUIDS AND OF STICK-SLIP-LIKE FLOW BEHAVIOR

SIEGFRIED HESS, ^[a]* SEBASTIAN HEIDENREICH, ^[a] PATRICK ILG, ^[a]
CHRIS GODDARD, ^[b] AND ORTWIN HESS ^[b]

ABSTRACT. Shear thickening, i.e. the increase of the viscosity with increasing shear rate as it occurs in dense colloidal dispersions and polymeric fluids is an intriguing phenomenon with a considerable potential for technical applications. The theoretical description of this phenomenon is patterned after the thermodynamic and mesoscopic modeling of the orientational dynamics and the flow behavior of liquid crystals in the isotropic and nematic phases, where the theoretical basis is well-established. Even there the solutions of the relevant equations recently yielded surprises: not only stable flow alignment and a periodic behavior (tumbling) are found as response to an imposed stationary shear flow but also irregular and chaotic dynamics occurs for certain parameter ranges. To treat shear-thickening fluids, a non-linear Maxwell model equation for the symmetric traceless part of the stress tensor has been proposed in analogy to the equations obeyed by the alignment tensor of nematics. The fluid-solid transition is formally analogous to the isotropic-nematic transition. In addition to shear-thickening and shear-thinning fluids, substances with yield stress can be modeled. Furthermore, periodic stick-slip-like motions and also chaotic behavior are found. In the latter cases, the instantaneous entropy production is not always positive. Yet it is comforting that its long-time average is in accord with the second law.

1. Introduction

The thermodynamic modeling of equilibrium properties and non-equilibrium phenomena in complex fluids and solids requires the treatment of *internal variables* and their coupling with the standard variables of thermo-hydrodynamics. In addition to general principles [1] the tensorial character of the internal variables has to be taken into account for specific applications, e.g. a vectorial variable is needed for dielectric relaxation [2] and the treatment of polarizable media [3]. In this article, second rank tensorial variables are considered, the alignment tensor and the stress tensor of nematic liquid crystals [4], [5] and the stress tensor of a nonlinear Maxwell model for shear-thickening fluids [6, 7] and substances with yield stress [8]. Similarities in the mathematical treatment of both cases but differences in the physical meaning as well as the mesoscopic derivation of the relevant equations and their microscopic interpretations are pointed out. In both cases a stationary flow can lead to a periodic and even to a chaotic response of the system [9], [10]. In nematic liquid crystal the periodic behavior is referred to as "tumbling" [11]. The periodic behavior of the nonlinear Maxwell model is reminiscent of the stick-slip motion seen in solid friction processes.

Sections 2 and 3 of this article are devoted to the flow alignment and viscous behavior of liquid crystals in their isotropic and nematic phases and to the nonlinear Maxwell model, respectively. More specifically, in section 2.1, relaxation equations and constitutive equations are stated which had been previously derived in the framework of irreversible thermodynamics and from a mesoscopic theory based on a generalized Fokker-Planck equation. Selected results are presented in section 2.2. In particular, the shear-flow induced transition isotropic-nematic and the chaotic behavior in the tumbling regime are discussed. The basics for the nonlinear Maxwell model are given in section 3.1. Results on shear-thickening and shear-thinning behavior, on stick-slip like behavior and its relevance for solid friction, as well as on rheo-chaos are presented in section 3.2. Section 3.3 is devoted to a discussion of the instantaneous entropy production which turns out to have occasionally the ‘wrong’ sign, for short times, for some values of the relevant parameters. Yet the long time average of the entropy production is in accord with the second law.

2. Flow Alignment and Viscous Behavior of Nematic Liquid Crystals

2.1. Relaxation equations and constitutive relations.

2.1.1. Alignment tensor. Fluids composed of effectively uniaxial particles with a molecular unit vector \mathbf{u} are characterized by an orientational distribution function $f(\mathbf{u}, t)$ [12, 13, 14, 15]. The relevant order parameter of a nematic liquid crystal is the 2nd rank alignment tensor

$$\mathbf{a} \equiv \sqrt{\frac{15}{2}} \langle \overline{\mathbf{u}\mathbf{u}} \rangle \equiv \int f(\mathbf{u}, t) \sqrt{\frac{15}{2}} \overline{\mathbf{u}\mathbf{u}} d^2u, \quad (1)$$

which is the anisotropic second moment characterizing the distribution. The symbol $\overline{\mathbf{x}}$ indicates the symmetric traceless part of a tensor \mathbf{x} . Frequently, the alignment tensor is also referred to as ‘ \mathbf{Q} -tensor’, sometimes as ‘ \mathbf{S} -tensor’. The symmetric traceless part of the dielectric tensor which gives rise to birefringence is proportional to the alignment tensor. Thus the shear flow induced modifications of the alignment can be detected optically [16].

For the special case of uniaxial symmetry (uniaxial phase) the alignment tensor \mathbf{a} can be parameterized by a scalar order parameter a and the director n , i.e., $\mathbf{a} = a(3/2)^{1/2} \overline{\mathbf{nn}}$, such that $a^2 = \mathbf{a} : \mathbf{a}$, and $-\sqrt{5}/2 \leq a = (3/2)^{1/2} \mathbf{a} : \overline{\mathbf{nn}} \leq \sqrt{5}$. The parameter a is therefore proportional to the Maier-Saupe order parameter $S_2 \equiv \langle P_2(\mathbf{u} \cdot \mathbf{n}) \rangle = a/\sqrt{5}$, where P_2 denotes the second Legendre polynomial.

The nonlinear relaxation equation for the alignment tensor was originally derived by (extended) irreversible thermodynamics [4]. The equation involves characteristic phenomenological coefficients viz. the relaxation time coefficients $\tau_a > 0$ and τ_{ap} , a dimensionless coefficient (shape factor) κ , the pseudo-critical temperature T^* , the nematic-isotropic transition temperature T_K with $T_K > T^*$, and the positive parameters A_0, B, C (with $C < 2B^2/(9A_0)$) of an amended Landau-de Gennes potential, with $\mathbf{a} : \mathbf{a} \leq a_{max}^2$ [17] $\Phi(\mathbf{a}) = (1/2)A(T)\mathbf{a} : \mathbf{a} - (1/3)\sqrt{6} B(\mathbf{a} \cdot \mathbf{a}) : \mathbf{a} - a_{max}^4 (C/4) \ln(1 - (\mathbf{a} : \mathbf{a})^2/a_{max}^4)$ with $A(T) = A_0(1 - T^*/T)$. The value of A_0 depends on the proportionality coefficient chosen between \mathbf{a} and $\langle \overline{u\mathbf{u}} \rangle$. The choice made in (1) implies $A_0 = 1$, cf. [4]. The coefficients, on the one hand, are linked with measurable quantities and, on the other hand, can be related to molecular quantities within the framework of a mesoscopic theory [12, 18, 19].

The equation of change for alignment tensor in the presence of a flow field \mathbf{v} is [4, 5]:

$$\frac{\partial \mathbf{a}}{\partial t} - 2\overline{\omega \times \mathbf{a}} - 2\kappa \overline{\mathbf{\Gamma} \cdot \mathbf{a}} + \tau_a^{-1} \mathbf{\Phi}(\mathbf{a}) = -\sqrt{2} \frac{\tau_{ap}}{\tau_a} \mathbf{\Gamma}, \quad (2)$$

where

$$\mathbf{\Phi}(\mathbf{a}) \equiv \partial \mathbf{\Phi} / \partial \mathbf{a} = A \mathbf{a} - \sqrt{6} B \overline{\mathbf{a} \cdot \mathbf{a}} + C (1 - (\mathbf{a} : \mathbf{a})^2 / a_{max}^4)^{-1} \mathbf{a} \mathbf{a} : \mathbf{a} \quad (3)$$

is symmetric traceless. The standard Landau-de Gennes expression is recovered when $\mathbf{a} : \mathbf{a} \ll a_{max}^2$, i.e. when the magnitude of the alignment is small compared with its limiting value a_{max} . The symbols $\mathbf{\Gamma}$ and ω denote the symmetric traceless part of the velocity gradient tensor (strain rate tensor) $\mathbf{\Gamma} \equiv \overline{\nabla \mathbf{v}}$, and the vorticity $\omega \equiv (\nabla \times \mathbf{v})/2$, respectively. In the case of a *simple shear flow*, often referred to as *plane Couette flow*, $\mathbf{v} = \dot{\gamma} y \mathbf{e}^x$ in x -direction, gradient in y -direction, and vorticity in z -direction, to be considered throughout the following analysis, these quantities simplify to $\mathbf{\Gamma} = \dot{\gamma} \overline{\mathbf{e}^x \mathbf{e}^y}$ and $\omega = -(1/2)\dot{\gamma} \mathbf{e}^z$. The unit vectors parallel to the coordinate axes are denoted by $\mathbf{e}^x, \mathbf{e}^y, \mathbf{e}^z$.

For lyotropic liquid crystals the concentration c of nonspherical particles in a solvent rather than the temperature determines the phase transition, i.e., in this case one has $A \propto (1 - c/c^*)$, where c^* is pseudo critical concentration [18]. An analysis based on the dynamics of the orientational distribution function is presented in [20, 21]. In Refs. [5, 9] the symbol σ was used instead of κ . The special values 0 and ± 1 for the coefficient κ in (2) correspond to corotational and codeformational time derivatives. From the solution of the generalized Fokker-Planck equation one finds, for long particles, $\kappa \approx 3/7 \approx 0.4$.

2.1.2. Pressure tensor. The pressure tensor \mathbf{p} consists of a hydrostatic pressure p , an antisymmetric part, and the symmetric traceless part $\overline{\mathbf{p}}$ referred to as friction pressure tensor [4]. The latter splits into a ‘isotropic’ contribution as already present in fluids composed of spherical particles or in fluids of non-spherical particles in an perfectly ‘isotropic state’ with zero alignment, and a part explicitly depending on the alignment tensor:

$$\overline{\mathbf{p}} = -2\eta_{iso} \mathbf{\Gamma} + \overline{\mathbf{p}_{al}}, \quad (4)$$

with [5, 9]

$$\overline{\mathbf{p}_{al}} = \frac{\rho}{m} k_B T \left(\sqrt{2} \frac{\tau_{ap}}{\tau_a} \mathbf{\Phi}(\mathbf{a}) - 2\kappa \overline{\mathbf{a} \cdot \mathbf{\Phi}(\mathbf{a})} \right). \quad (5)$$

The symmetric traceless part of the stress tensor to be used later is just $-\overline{\mathbf{p}}$. In equilibrium one has $\mathbf{\Phi}(\mathbf{a}) = 0$ and consequently $\overline{\mathbf{p}_{al}} = 0$. The occurrence of the same coupling coefficient τ_{ap} in (5) as in (2) is due to an Onsager symmetry relation. For results on the rheological properties in the isotropic and in the nematic phases with stationary flow alignment, following from (2) and (5) see [4, 5, 9]. Here, the attention is focused on the rheology in the tumbling and in complex dynamic states.

2.1.3. Scaled variables and model parameters. The equations (2) and (5) can be rewritten in scaled variables [5, 9] which are convenient for the theoretical analysis. Firstly, the alignment tensor is expressed in units of the value of the order parameter at the isotropic-nematic phase transition, $a_K = \frac{2B}{3C}$ occurring at the temperature $T_K > T^*$. With the temperature variable $\vartheta \equiv \frac{9}{2} \frac{AC}{B^2} = \frac{1-T^*/T}{1-T^*/T_K}$ the temperature dependence of the uniaxial equilibrium alignment is $a_{eq} = 0$ for $\vartheta \geq 9/8$ (isotropic phase) and

$a_{\text{eq}}/a_K = \frac{1}{4}(3 + \sqrt{9 - 8\vartheta})$, for $\vartheta < 9/8$ (nematic phase), when $a_{\text{max}} \geq 2.5$. The equilibrium phase coexistence temperature corresponds to $\vartheta = 1$. The values $\vartheta = 9/8$ and $\vartheta = 0$ are the upper and lower limits of the metastable nematic and isotropic states, respectively. The quantity $\delta_K = 1 - T^*/T_K$ which sets a scale for the relative difference of the temperature from the equilibrium phase transition is known from experiments to be of the order 0.1 to 0.001. On the other hand, it is related to the coefficients occurring in the potential function according to $\delta_K = \frac{2}{9} \frac{B^2}{A_0 C} = \frac{1}{2} a_K^2 \frac{C}{A_0}$.

The derivative Φ of the potential function in (2) can be written as $\Phi = \Phi_{\text{ref}} \Phi^*$ with $\Phi_{\text{ref}} = a_K \frac{2}{9} \frac{B^2}{C} = a_K \delta_K A_0$, $\mathbf{a}^* = \mathbf{a}/a_K$, and

$$\Phi^*(\mathbf{a}^*) = \vartheta \mathbf{a}^* - 3\sqrt{6} \sqrt{\mathbf{a}^* \cdot \mathbf{a}^*} + 2(1 - (\mathbf{a}^* : \mathbf{a}^*)^2 / (a_{\text{max}}^*)^4)^{-1} \mathbf{a}^* \mathbf{a}^* : \mathbf{a}^*. \quad (6)$$

Clearly, the variable ϑ suffices to characterize the equilibrium behavior determined by $\Phi = 0$. It should be mentioned that ϑ can be also be interpreted as a density or concentration variable according to $\vartheta = (1 - c/c^*) / (1 - c_K/c^*)$ where c stands for the concentration in lyotropic liquid crystals. For the full nonequilibrium system, times and shear rates are made dimensionless with a convenient reference time. The relaxation time of the alignment in the isotropic phase is $\tau_a A_0^{-1} (1 - T^*/T)^{-1}$ showing a pre-transitional increase. This relaxation time, at coexistence temperature T_K , is used as a reference time $\tau_{\text{ref}} = \tau_a (1 - T^*/T_K)^{-1} A_0^{-1} = \tau_a \delta_K^{-1} A_0^{-1} = \tau_a \frac{9C}{2B^2} = \tau_a a_K \Phi_{\text{ref}}^{-1}$. The shear rates are expressed in units of τ_{ref}^{-1} . The scaled shear rate, being a product of the true shear rate and the relevant relaxation time, is also referred to as ‘Deborah-number’. Instead of the ratio τ_{ap}/τ_a , the parameter

$$\lambda_k = -(2/3)\sqrt{3} \frac{\tau_{\text{ap}}}{\tau_a} a_K^{-1} \quad (7)$$

is used. As was shown previously [4, 5, 9], the coefficients τ_a and τ_{ap} are proportional to the Ericksen-Leslie [22] viscosity coefficients γ_1 and γ_2 , respectively. The present theory applies both for the isotropic and for the nematic phase. The Ericksen-Leslie theory follows from the present approach when the alignment tensor is uniaxial and when the effect of the shear flow on the magnitude of the order parameter can be disregarded. Then it suffices to use a dynamic equation for the ‘director’ which is a unit vector parallel to the principal axis of the alignment tensor associated with its largest eigenvalue. This is a good approximation deep in the nematic phase and for small shear rates. For intermediate and large shear rates and, in particular, in the vicinity of the isotropic-nematic phase transition, the tensorial description is essential. The ‘tumbling coefficient’ $\lambda = -\gamma_2/\gamma_1 = \lambda(a_{\text{eq}})$ is given by $\lambda_{\text{eq}} = \lambda_k \frac{a_K}{a_{\text{eq}}} + \frac{1}{3} \kappa$, where a_{eq} is recalled as the equilibrium value of the alignment in the nematic phase. Thus λ_{eq} is equal to λ_k at the transition temperature provided that $\kappa = 0$. In the limit of small shear rates $\dot{\gamma}$, the tumbling parameter is related to the Jeffrey tumbling period [24]. Within the Ericksen-Leslie description, the flow alignment angle χ in the nematic phase is determined by $\cos(2\chi) = -\gamma_1/\gamma_2 = 1/\lambda_{\text{eq}}$. A stable flow alignment, at small shear rates, exists for $|\lambda_{\text{eq}}| > 1$ only. For $|\lambda_{\text{eq}}| < 1$ tumbling and an even more complex time dependent behavior of the orientation occur. The quantity $|\lambda_{\text{eq}}| - 1$ can change sign as function of the variable ϑ . For $|\lambda_{\text{eq}}| < 1$ and in the limit of small shear rates $\dot{\gamma}$, the Jeffrey tumbling period [24] is related to the Ericksen-Leslie tumbling parameter λ_{eq} by $P_J = 4\pi / (\dot{\gamma} \sqrt{1 - \lambda_{\text{eq}}^2})$, for a full rotation of the director.

Both λ_k and κ are model parameters. The first one is essential for the coupling between the alignment and the viscous flow. The second one influences the orientational behavior quantitatively but does not seem to affect it in a qualitative way for a simple shear flow. Mesoscopic theories [12, 19, 25] indicate that $\kappa \neq 0$. The value of κ and also of a_{max} matters for vorticity free flow fields, e.g. for the planar biaxial 4-roller flow and the uniaxial elongational flow.

The stress tensor (5) associated with the alignment is related to the relevant quantities expressed in terms of scaled variables by $\frac{\rho}{m} k_B T a_K \Phi_{\text{ref}} \frac{\sqrt{3}}{2} \lambda_k \tilde{\Phi}$, $\tilde{\Phi} = \Phi^* + \frac{2\kappa}{3\lambda_k} \sqrt{6} \overline{\mathbf{a}^* \cdot \Phi^*}$, where $\mathbf{a}^* = \mathbf{a}/a_K$ and $\Phi^* = \Phi/\Phi_{\text{ref}}$. The dimensionless shear stress Σ^{al} associated with the alignment is defined by $\Sigma^{\text{al}} \equiv \frac{2}{\sqrt{3}} \lambda_k^{-1} \tilde{\Phi}$. Then one has $-\overline{\mathbf{p}} = \sqrt{2} G_{\text{al}} \Sigma^{\text{al}}$, $G_{\text{al}} = \frac{3}{4} \frac{\rho k_B T}{m} \lambda_k^2 \delta_K A_0 a_K^2$, where G_{al} is a shear modulus associated with the alignment contribution to the stress tensor, and the product $A_0 a_K^2$ is essentially one parameter entering the theoretical expressions. The quantity $\eta_{\text{iso}} = G_{\text{al}} \tau_a$ serves as a reference value for the viscosity. With the scaling used here, the dimensionless (first) Newtonian viscosity, in the isotropic phase, is $\eta_{\text{New}}^* = 1 + \eta_{\text{iso}}^*$ with $\eta_{\text{iso}}^* = \eta_{\text{iso}}/\eta_{\text{ref}}$. For high shear rates the dimensionless viscosity $H = \eta^*$ approaches the second Newtonian viscosity $H_{\text{iso}} = \eta_{\text{iso}}^*$. The total deviatoric (symmetric traceless) part of the stress tensor, in units of G_{al} , is denoted by σ . In terms of the quantities introduced here it is given by, cf. (4),

$$G_{\text{al}} \sigma = -\overline{\mathbf{p}} = 2 \eta_{\text{iso}} \mathbf{\Gamma} - \overline{\mathbf{p}} = 2 \eta_{\text{iso}} \mathbf{\Gamma} + \sqrt{2} G_{\text{al}} \Sigma^{\text{al}}. \quad (8)$$

Quantities in reduced units are denoted by the same symbols as the original ones, unless ambiguities could arise.

2.1.4. Special geometry. The symmetric traceless alignment tensor has five independent components. It can be expressed in a standard [26] ortho-normalized tensor basis as follows: $\mathbf{a} = \sum_{k=0}^4 a_K \mathbf{T}^k$, with $\mathbf{T}^0 \equiv \sqrt{3/2} \overline{\mathbf{e}^z \mathbf{e}^z}$, $\mathbf{T}^1 \equiv \sqrt{1/2} (\mathbf{e}^x \mathbf{e}^x - \mathbf{e}^y \mathbf{e}^y)$, $\mathbf{T}^2 \equiv \sqrt{2} \overline{\mathbf{e}^x \mathbf{e}^y}$, $\mathbf{T}^3 \equiv \sqrt{2} \overline{\mathbf{e}^x \mathbf{e}^z}$, $\mathbf{T}^4 \equiv \sqrt{2} \overline{\mathbf{e}^y \mathbf{e}^z}$, where $\mathbf{e}^{x,y,z}$ are unit vectors parallel to the coordinate axes. The flow velocity is chosen to be in x -direction with its gradient in y -direction. The orthogonality relation and the expression for the coefficients a_k are given by $\mathbf{T}^i : \mathbf{T}^k = \delta_{ik}$ and $a_k = \mathbf{a} : \mathbf{T}^k$. Using these basis tensors, we obtain a system of five ordinary differential equations from (2), cf. [9].

The corresponding expansion with respect to the basis tensors and the component notation can be used for the other second rank irreducible tensors. The expressions for the (dimensionless) shear stress σ_{xy} and the normal stress differences $N_1 = \sigma_{xx} - \sigma_{yy}$ and $N_2 = \sigma_{yy} - \sigma_{zz}$ in terms of the dimensionless tensor components $\Sigma_i \equiv \Sigma^{\text{al}} : \mathbf{T}^i$, are

$$\sigma_{xy} = \eta_{\text{iso}} \dot{\gamma} + \Sigma_2, \quad N_1 = 2 \Sigma_1, \quad N_2 = -\sqrt{3} \Sigma_0 - \Sigma_1. \quad (9)$$

In reduced units, the shear viscosity $H = \eta^*$ is

$$H = \sigma_{xy}/\dot{\gamma} = \eta_{\text{iso}} + \Sigma_2/\dot{\gamma}. \quad (10)$$

2.2. Selected results.

2.2.1. Shear-flow-induced phase transition isotropic-nematic. For large values of ϑ , typical for the isotropic phase, terms nonlinear in the alignment can be disregarded. Solutions for a stationary situation e.g. are given in [9]. The viscosity shows a shear-thinning behavior.

Still in the isotropic phase, but closer to the phase transition temperature $\vartheta = 1$, a shear induced transition to the nematic phase occurs. This is seen in the discontinuity of the viscosity plotted versus the shear rate in Fig.1 for $\vartheta = 1.3$, $\lambda_k = 1.25$, $\kappa = 0$, $\eta_{\text{iso}} = 0.1$, and $a_{\text{max}} \gg 1$.

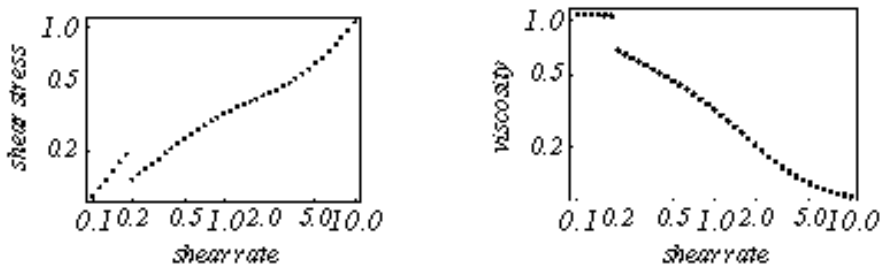


FIGURE 1. The shear stress and the viscosity versus the shear rate in the temperature range where shear flow induces a transition from the isotropic into the nematic phase. For the model parameters see the text.

Based on the equations presented here, a shear-flow-induced isotropic-to-nematic phase transition has been predicted theoretically quite some time ago [4, 27]. This phenomenon has been observed in lyotropic liquid crystals, in particular with wormlike micelles [28] and in side-chain liquid-crystalline polymers [29]. The latter case has been treated by a theory involving two alignment tensors [30].

2.2.2. Orbits for regular and chaotic behavior. Instead of analyzing the components of the alignment and stress tensors as functions of the time, it is more instructive to produce ‘orbits’ or ‘phase portraits’ where one component is plotted versus another one. The true alignment orbit is a curve in five-dimensional space, the two-dimensional orbits to be shown are projections on various planes. Usually, the notion ‘phase portrait’ is applied to plots of a ‘velocity’ (time derivative) versus a ‘coordinate’. Here a plot of a normal stress difference versus the shear stress is referred to as ‘rheological phase portrait’. In a stationary state, the alignment orbits consist of a single point, relatively simple curves indicate the transient behavior during the approach towards the asymptotic state. The symmetry adapted components a_0, a_1, a_2 of the alignment tensor as well as the shear stress and the normal stress differences approach single non-zero values whereas the symmetry-breaking components a_3, a_4 tend to zero. The orbits look drastically different for periodic and for chaotic solutions to be presented next, in an order as encountered with increasing shear rates, at $\vartheta = 0.0$, a temperature just below the transition into the nematic phase.

Examples for the rheological properties are shown in Fig. 2. The parameters are $\vartheta = 0.0$, $\lambda_k = 1.05$, $\kappa = 0.4$ at the shear rate 4.2. The left graph pertains to the start up from an initial state where all components of the alignment tensor are small but not zero, time is up to 125. The right graph is for times from start to 500. First a focus with a negative first normal stress difference is approached. This state is not stable. The system evolves to a state with a positive normal stress difference. A strange attractor is observed in this region. Occasionally the state with negative normal stress is revisited. The largest Lyapunov coefficient, determined over much longer times, is positive indicating a chaotic behavior.

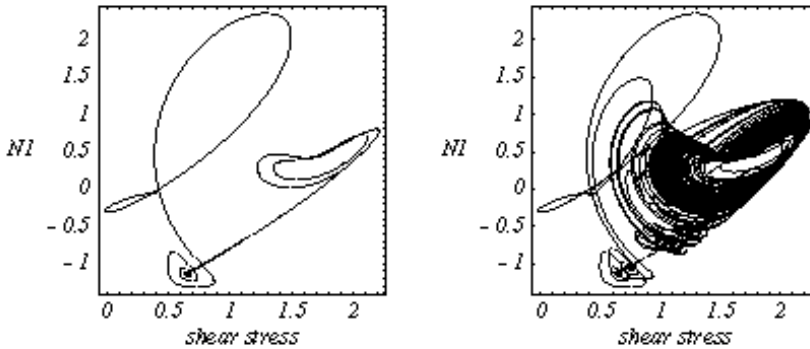


FIGURE 2. Rheological phase portrait showing the first normal stress difference versus the shear stress at start up and at later times in the chaotic regime. For the model parameters see the text.

At high shear rates a flow aligned state is reached with orbits and rheological phase portraits which are rather simple compared with those shown above.

3. Nonlinear Maxwell model

3.1. Ingredients and basics. The symmetric traceless (deviatoric) part $\overline{\sigma}$ of the stress tensor σ is decomposed into a contribution associated with the "internal structure" for which the nonlinear Maxwell model equations are formulated and contribution linked with a "second newtonian" viscosity η_∞ reached at high shear rates:

$$\overline{\sigma} = \sqrt{2} G \pi + 2 \eta_\infty \Gamma . \quad (11)$$

The quantity G is a reference value for a shear modulus such that π is a dimensionless "friction stress tensor". An obvious choice for G (which is not needed now) is either the high-frequency shear modulus or the reference pressure $p_{ref} = nk_B T$ where n and T are the number density and the temperature. The factor $\sqrt{2}$ has been inserted for convenience, the factor 2 in (11) is conventional. As before, the symbol $\overline{\cdot}$ indicates the symmetric traceless part of a tensor, e.g. in Cartesian tensor notation, $\overline{\sigma_{\mu\nu}} = \frac{1}{2}(\sigma_{\mu\nu} + \sigma_{\nu\mu}) - \frac{1}{3}\sigma_{\lambda\lambda}\delta_{\mu\nu}$, where $\delta_{\mu\nu}$ is the unit tensor.

When π obeys the Maxwell model equation, the constitutive relation (11) is referred to as Jeffrey model. In following a generalization of the Maxwell model is used. When π is interpreted as the second moment of the velocity distribution function of a gas, an equation of this type can be and has been derived from the nonlinear Boltzmann equation [31], [32]. For a simple liquid, the dominant contribution to the friction stress is the virial tensor for which a generalized Maxwell equation can be derived from a kinetic equation of Kirkwood-Smoluchowski type for the pair correlation function [33]. For polymeric fluids, π can be linked with the second moment of a segment orientation function or with the second rank conformation tensor.

3.1.1. Relaxation equation for the stress tensor. The friction stress tensor is assumed to obey the generalized Maxwell equation [8, 10]

$$\frac{\partial \pi}{\partial t} - 2\overline{\omega \times \pi} - 2\kappa \overline{\Gamma \cdot \pi} + \tau_0^{-1} \Phi(\pi) = -\sqrt{2} \Gamma, \quad (12)$$

Here τ_0 is a relaxation time coefficient. The tensor $\Phi = \partial \Phi / \partial \pi$ is the derivative of a "potential" function Φ with respect to the deviatoric stress tensor π . The scalar function $\Phi = \Phi(I_2, I_3)$ depends on the second and third order scalar invariants, written in component notation, $I_2 = \pi_{\mu\nu} \pi_{\mu\nu}$, $I_3 = \sqrt{6} \pi_{\mu\nu} \pi_{\nu\lambda} \pi_{\lambda\mu} = 3\sqrt{6} \det(\pi)$.

The "linear" Maxwell model pertains to the simplest choice for the potential function Φ , viz.: $\Phi = \frac{1}{2} A I_2$, with a dimensionless coefficients $A > 0$. This implies $\Phi = A \pi$. For $\kappa = 0$ the time change in (12) is governed by the corotational time derivative. Thus the relaxation equation (12) reduces to the *Jaumann-Maxwell* model with the Maxwell relaxation time $\tau = \tau_0 A^{-1}$. The Newtonian viscosity, attained for small shear rates is $\eta = \eta_{New} := G \tau + \eta_\infty = G \tau_0 A^{-1} + \eta_\infty$.

For $\kappa = 1$ or $\kappa = -1$ the time change corresponds to that of a codeformational time derivative. Just as in the relaxation equation for the alignment tensor (2), κ is regarded as an additional model parameter.

In the absence of a flow the stationary solution of (12) is $\Phi = 0$. In a fluid state one has $\pi = 0$ and this is a stable solution corresponding to the absolute minimum of the potential function Φ . The quantity $\Phi = 0$ being a nonlinear function of the stress also has solutions with $\pi \neq 0$ for certain ranges of the model parameters. If such a solution is (locally) stable the system possesses a yield stress.

3.1.2. Potential function. When terms up to sixth order in the stress tensor are taken into consideration the ansatz for the potential function is $\Phi = \frac{1}{2} A I_2 - \frac{1}{3} B I_3 + \frac{1}{4} C I_2^2 + \frac{1}{5} D I_2 I_3 + \frac{1}{6} E I_3^2 + \frac{1}{6} F I_3^2$, where the dimensionless coefficients A, B, C, D, E, F are model parameters. Notice that the derivatives of I_2 and I_3 with respect to $\pi_{\mu\nu}$ are, in component notation, $2\pi_{\mu\nu}$ and $3\sqrt{6} \overline{\pi_{\mu\lambda} \pi_{\lambda\nu}}$, respectively.

In analogy to the equations governing the alignment tensor of nematic liquid crystals, the simple ansatz with terms up to fourth order in the stress tensor is made. This means $D = E = F = 0$ and $C > 0$. Then one has

$$\Phi = A \pi - \sqrt{6} B \overline{\pi \cdot \pi} + C \pi(\pi : \pi). \quad (13)$$

For the special case where the stress tensor is uniaxial one has $\pi = \sqrt{\frac{3}{2}} \pi_0 \overline{\mathbf{nn}}$. Here \mathbf{n} is a unit vector \mathbf{n} parallel to the symmetry axis. Then the potential function reduces to $\Phi = \frac{1}{2}A\pi_0^2 - \frac{1}{3}B\pi_0^3 + \frac{1}{4}C\pi_0^4$. In this case $\Phi = 0$ corresponds to $\pi_0(A - B\pi_0 + C\pi_0^2) = 0$. Solutions of this equation are $\pi_0 = 0$, corresponding to a fluid state and $\pi_0 = B/(2C) \pm \sqrt{B^2/(4C^2) - A/C}$, when $A \leq B^2/(4C)$. The case $\pi_0 \neq 0$ in the absence of a flow corresponds to a (metastable) solid state with a yield stress.

In the Landau theory for (equilibrium) phase transitions the assumption is made that A depends on the temperature T or on the density ρ according to $A = A_0(1 - T_0/T)$ or $A = A_0(1 - \rho/\rho_0)$ with characteristic temperature T_0 or density ρ_0 . Here such a specific dependence of A is not needed but it is presupposed that A decreases with decreasing temperature and increasing density. Furthermore one assumes $A_0 > 0$, $B \neq 0$, $C > 0$, $\approx const.$

3.1.3. Scaled variables. Scaled variables are introduced in order to characterize the importance of the terms nonlinear in the stress by a single model parameter. Following, as in [8], the procedure used for the isotropic-nematic phase transition in liquid crystals [4, 9] and as treated above, the components of π are expressed in units of $\pi_c = \frac{2}{3} \frac{B}{C}$, $\pi = \pi_c \pi^*$. With $A = A^* A_c$, $A_c := 2B^2(9C)^{-1}$, $\tau_c = \tau_0 A_c^{-1} = \tau_0 (\frac{1}{2} C \pi_c^2)^{-1}$, $C > 0$; and $t = \tau_c t^*$, $\Gamma_{\mu\nu} = \tau_c \gamma_{\mu\nu}$, the model coefficients B and C no longer appear explicitly in the relaxation equations. In the following, the scaled variables are denoted by the same symbol as the original variables when no danger of confusion is expected, e.g. $\pi_{\mu\nu}^* \rightarrow \pi_{\mu\nu}$, $t^* \rightarrow t$. Then we have

$$\Phi \rightarrow A^* \pi - 3\sqrt{6} \overline{\pi \cdot \pi} + 2\pi(\pi : \pi). \quad (14)$$

For the special case of a uniaxial stress the scaled potential function is $\Phi(\pi) = \frac{1}{2}A^*\pi_0^2 - \pi_0^3 + \frac{1}{2}\pi_0^4$, and $\Phi = 0$ corresponds to $\pi_0(A^* - 3\pi_0 + 2\pi_0^2) = 0$. For $A^* = 1$ one has 'phase coexistence', i.e. $\Phi(0) = \Phi(1)$.

The coefficient A^* determines whether terms of higher order in the components of the pressure tensor are of relevance ($A^* \approx 1$) or not ($A^* \gg 1$). It is assumed that A^* depends strongly on the temperature T or on the number density ρ of a dispersion in a way typical for a Landau-type theory of a phase transition. More specifically, it is expected that A^* decreases with decreasing T or with increasing ρ . The Newtonian viscosity increases with decreasing T or increasing n due to the increase of the relaxation time τ . The fluid state "coexists" with a state possessing a yield stress at $A^* = 1$. For $A^* > 1.125$ no stationary solution with non-zero values of the tensor π exists in equilibrium.

In general, the shear stress has 5 components. The basis tensors introduced above are again used and the components of the (dimensionless) stress tensor are denoted by π_i , $i = 0, 1, 2, 3, 4$. In [8] the subscripts "+" and "-" were used instead of "2" and "1". For a plane Couette geometry it frequently suffices to consider the 3 components π_2, π_1, π_0 . For some ranges of the relevant model parameters and shear rates the two additional components π_3, π_4 also are needed for the Couette symmetry. In this case the components π_3, π_4 are referred to as symmetry-breaking components.

The nonlinear Maxwell model equation (12) with (13) is equivalent to 5 equations for the components π_i , cf.[10].

3.1.4. Viscosity and Stress Components. The non-Newtonian viscosity η is the ratio of the shear stress and the applied shear rate, thus $\sigma_{xy} = \eta\dot{\gamma} = G H \Gamma$. In the following, results for the viscosity are presented in units the reference viscosity $\eta_{ref} = G\tau_c$.

The dimensionless viscosity coefficient H is determined by $H = \pi_c \pi_2 / \Gamma + H_\infty$, $H_\infty = \eta_\infty / \eta_{ref}$. Similarly, the scaled (dimensionless) shear stress

$$\sigma^* = H\Gamma = \pi_c \pi_2 + H_\infty \Gamma \quad (15)$$

and the scaled (dimensionless) first and second normal stress differences

$$N_1^* = (\sigma_{xx} - \sigma_{yy})/G = 2\pi_c \pi_1, \quad N_2^* = (\sigma_{yy} - \sigma_{zz})/G = -\pi_c (\pi_1 + \sqrt{3}\pi_0) \quad (16)$$

are used. Here, the dimensionless scaled shear rate is denoted by Γ . In graphs σ^* and N_1^* are also denoted by σ and ν . According to standard wisdom, the entropy production has to be positive, at least in a stationary situation and when averaged over long times. This condition is fulfilled when $\eta > 0$, and hence $H > 0$. For a discussion of the entropy production see section 3.3.

For $A^* > 1.125$ and for very small shear rates, the stationary value of the dimensionless viscosity is its newtonian limit

$$H = H_{New} := 1/A^* + H_\infty.$$

3.1.5. Tumbling parameter. In nematic liquid crystals, the alignment tensor may be stationary or not in the presence of a steady shear flow depending on whether the "tumbling parameter" λ is larger or smaller than 1 [11]. Comparison of the nonlinear Maxwell model with the relaxation equations governing the alignment tensor shows that the parameter π_c is related to the model parameter λ_K of [9] and used above, by $\lambda_K = 2/(\sqrt{3}\pi_c)$. The tumbling parameter, only defined for $A^* < 1.125$, is given by

$$\lambda = 2 \left(\sqrt{3}\pi_c \pi_{eq} \right)^{-1} + \kappa/3, \quad \pi_{eq} = (3 + \sqrt{9 - 8A^*})/4. \quad (17)$$

For $\pi_c = 1$ and $\kappa = 0$, the parameter values to be used in the following studies, one has $\lambda < 1$ for $A^* \approx 0.8$. Thus stationary solutions exist for $A^* > 0.8$ whereas a time dependent, oscillatory or irregular response is expected for $A^* < 0.8$. For nematics with $\lambda^2 < 1$, the "tumbling frequency" $\omega_{tumb} = (1/2)\Gamma\sqrt{1 - \lambda^2}$ has been defined. In general, it just gives an estimate of an oscillation frequency in a more complex dynamical behavior.

3.2. Results.

3.2.1. Stationary solution, shear thickening behavior. First, we confine our attention to the range of model parameters where we know that stationary solutions exist for a constant applied shear rate. The symmetry breaking components π_3 and π_4 vanish in this case. Analytic solutions were given in [8], here the main emphasis is on numerical solutions the nonlinear relaxation equations. The "NDSolve" routine of Mathematica is used for the computations.

The non-Newtonian viscosity as displayed in Fig.3 shows the transition from a simple shear-thinning behavior to a more complex shear-thickening behavior followed by shear-thinning at higher shear rates when the control parameter A^* decreases. More specifically, the viscosity H is shown as function of the shear rate Γ for $A^* = 1.25, 1.5, 2.0, 5.0$, and $\pi_c = 1.0, \kappa = 0.0, H_\infty = 0.1$. The curve with the largest (smallest) viscosity at small

shear rates pertains to $A^* = 1.25$ ($A^* = 5.0$). The curves represent the analytic solutions given in [8], the points stem from the long time limit of the numerical solutions of the relaxation equations for the stress components.

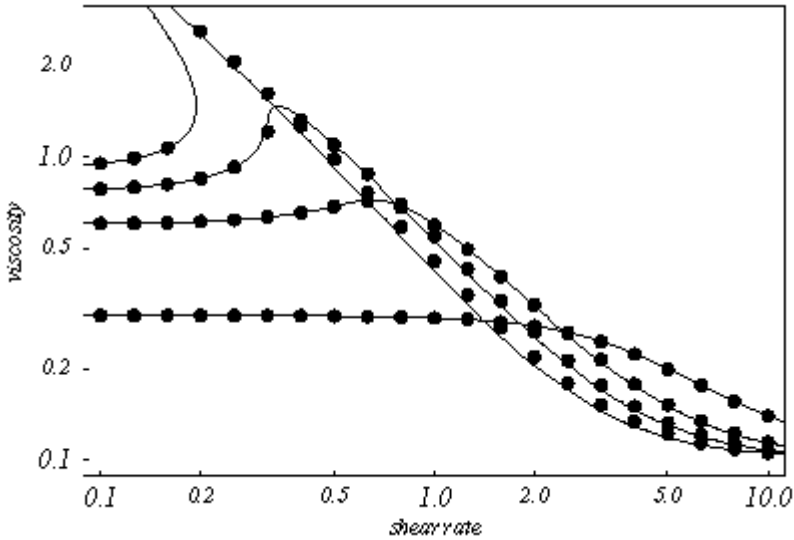


FIGURE 3. The viscosity as function of the shear rate in the shear-thinning shear-thickening regime

3.2.2. Stick-slip like behavior and solid friction. An example for the non-steady reponse of the system to an applied steady shear, essentially of stick-slip type, is presented in Fig.4 for the model parameters $\pi_c = 1.0$, $\kappa = 0.0$, $H_\infty = 0.1/A^*$, and for $A^* = 0.25, 0.35, 0.42$, from top to bottom, at the shear rate 3.2. Such a behavior is strikingly similar to that one seen in solid friction processes [34] where the friction force is studied as function of the time for many repetitions of beach wood sliding over iron, at a constant speed. Notice that the friction force is proportional to the shear stress. When the plastic flow responsible for the friction occurs in a layer which is approximately constant, a constant velocity corresponds to a constant velocity gradient as considered here. In the experiment, initially curves are observed which are similar to the lowest one, pertaining to $A^* = 0.42$. Due to the wear, an increasing number of iron particles are transferred as inclusions into the wood. This corresponds to an decrease of A^* and leads to a stick-slip behavior as displayed in the graph.

3.2.3. Rheo-chaos. The irregular dynamic response of the shear stress is referred as *rheo-chaos*. The term was originally introduced in [35] for a theoretical model different from those discussed here. Both tumbling liquid crystals, as treated above, and the nonlinear Maxwell show chaotic behavior. Examples for the later case are presented in [10]. Here, in Fig.5 the shear stress $\sigma = \pi_2 \pi_c + H_\infty \Gamma$, the first normal stress difference $\nu = N_1 = \pi_1 \pi_c$

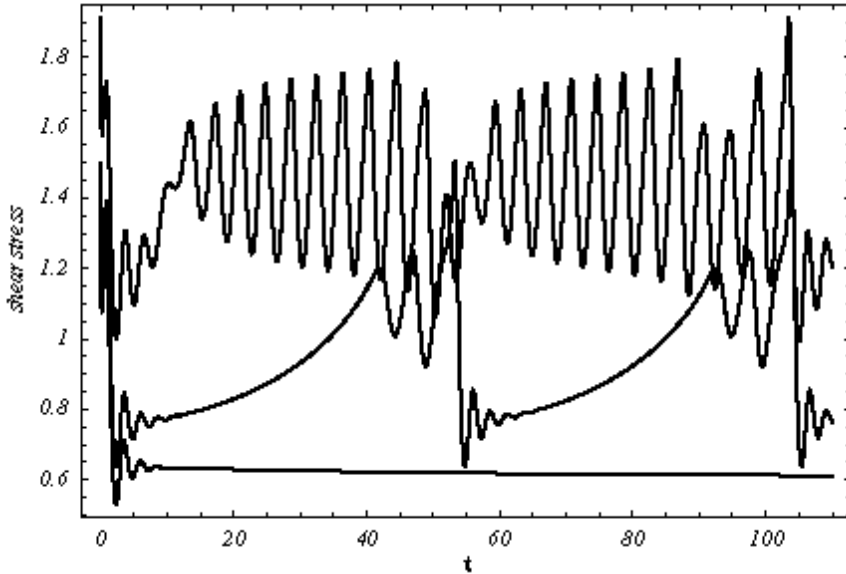


FIGURE 4. The shear stress as function of the time at the shear rate 3.2 for $A^* = 0.25, 0.35, 0.42$, top to bottom.

and $q = \pi_0$ are displayed in a 3-dimensional phase plot for $A^* = 0.33$, $\kappa = 0$, $H_\infty = 0.1$ and for the shear rate $\Gamma = 3.25$. The left graph, for times 0 to 100 shows the approach to a fix point which, however, is instable. The right graph, for times 0 to 200 indicates the emergence of a strange attractor, typical for a chaotic behavior.

3.3. Entropy production. The theory governing the dynamics of liquid crystals was formulated such that the entropy production is always positive [4]. The situation is different for the nonlinear Maxwell model [8, 10] in the parameter range where periodic solutions exist. The specific entropy production Θ_π (per unit mass) associated with the symmetric traceless shear stress tensor $\pi_{\mu\nu}$ and its time change is given by [10]

$$(m/k_B)\Theta_\pi = \pi_{\mu\nu} \sqrt{2} \gamma_{\mu\nu} - \Phi_{\mu\nu} \frac{d\pi_{\mu\nu}}{dt}. \quad (18)$$

Here the reference value $nk_B T$ has been used for G_{ref} , m is the mass of a particle and $\gamma_{\mu\nu}$ is recalled as the symmetric traceless (deviatoric) part of the velocity gradient tensor. The total entropy production Θ contains an additional contribution $2\eta_\infty \gamma_{\mu\nu} \gamma_{\mu\nu}$. For the plane Couette geometry considered here, the scaled entropy production Θ^* , defined by $\Theta = (k_B/m)\tau_c^{-1} \Theta^*$, is given

$$\Theta^* = \pi_c \left(\pi_2^* \Gamma - A_c \Phi_{\mu\nu}^* \frac{d\pi_{\mu\nu}^*}{dt^*} \right) + H_\infty \Gamma^2 \quad (19)$$

with $A_c = 0.5 \pi_c^2 C$.

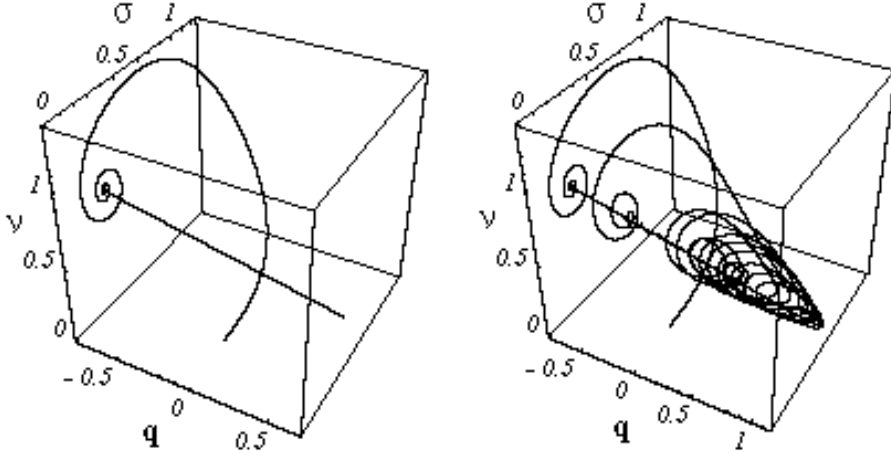


FIGURE 5. The shear stress σ , the first normal stress difference $\nu = N_1$ and $q = \pi_0$ in a 3-dim phase plot. The left and right graphs are for times 0 to 100 and 0 to 200, respectively. For the model parameters see the text.

The standard assumption made in irreversible thermodynamics is $\Theta > 0$. For a stationary situation, this simply means that the viscosity is positive. The present model leads to such a behavior, even in the nonlinear flow regime, provided that a stable stationary solution exists. For time dependent processes, the inequality $\Theta > 0$ need not to be obeyed at all instances. The second law of thermodynamics just requires that the long time average $\langle \Theta \rangle$ of the entropy production be positive. Theoretical and recently also experimental studies [36] reveal that the instantaneous value of Θ can be negative, for a "short" duration which is longer for small systems. In non-equilibrium molecular dynamics (NEMD) computer simulations [37] of fluids the shear stress can have the "wrong" sign which means $\Theta < 0$, over times that are of the order of microscopic relaxation times. In the case of stick-slip flow in sheared solids subjected to small shear rates, somewhat longer durations occur [37] for this phenomenon. In the present model, Θ can be negative over "mesoscopic" times determined by the "tumbling" period in the case a non-steady reponse of the system. An example for such a behavior is shown in [10]. In the chaotic regime, where the applied shear rates are ± 3.2 , also the instantaneous entropy production Θ is positive.

The temporary occurrence of $\Theta < 0$ and of a shear stress with the wrong sign is prevented when the second newtonian viscosity, i.e. the quantity H_∞ is large enough. Notice that this parameter does not affect the dynamics of the part of the stress tensor which obeys the nonlinear Maxwell model equations. Such a remedy is not very satisfactory. One either has to accept the occurrence of $\Theta < 0$ or one should reformulate the model such that one has always $\Theta > 0$, even for $H_\infty = 0.0$. A proposal how this can be done is made in [10].

4. Conclusions

In this article, the analysis was restricted to a situation with a spatially homogeneous velocity gradient as in an ideal plane Couette flow. In general, one has to deal with a spatially inhomogeneous alignment and velocity gradients as well as with the onset of a secondary flow which is typical for non-newtonian fluids. Thus the equation for the alignment tensor and the stress tensor of the nonlinear Maxwell model have to be amended as indicated in [5, 10]. Furthermore the full hydrodynamic problem has to be solved. Here particle methods as formulated in [38] can be useful.

Acknowledgements

This work started, proceeded and was completed under the auspices of the SFB 335 "Anisotrope Fluide", SFB 605 "Elementarereignisse" and SFB 448 "Mesoskopisch strukturierte Verbundsysteme". We thank M. Ellero, M. Kröger and I. Stankovic for helpful discussions. Support via an EPSRC Doctoral Training Grant is gratefully acknowledged.

References

- [1] G.A. Maugin and W. Muschik, *J. Non-Equilib. Thermodyn.* **19**, 217; 250 (1994).
- [2] L. Restuccia and G.A. Kluitenberg, *Physica A* **154**, 157 (1988); *J. Non-Equilib. Thermodyn.* **15**, 335 (1990).
- [3] M. Francaviglia, L. Restuccia and P. Rogolino, *J. Non-Equilib. Thermodyn.* **29**, 221 (2004).
- [4] S. Hess, *Z. Naturforsch.* **30a**, 728, 1224 (1975); **31a**, 1507 (1976).
- [5] S. Hess and I. Pardowitz, *Z. Naturforsch.* **36a**, 554 (1981); C. Pereira Borgmeyer and S. Hess, *J. Non-Equilib. Thermodyn.* **20**, 359 (1995).
- [6] H. M. Laun, R. Bung, and F. Schmidt, *J. Rheol.* **35** (1991) 999; H. M. Laun, R. Bung, S. Hess, W. Loose, O. Hess, K. Hahn, E. Hädicke, R. Hingmann, F. Schmidt, and P. Lindner, *J. Rheol.* **36** (1992) 743.
- [7] E. Michel, J. Appell, F. Molino, J. Kiefer, and G. Porte, *J. Rheol.* **45** (2001) 1465.
- [8] O. Hess and S. Hess, *Physica A* **207**, 517 (1994).
- [9] G. Rienäcker, M. Kröger, and S. Hess, *Phys. Rev. E* **66**, 040702(R) (2002); *Physica A* **315**, 537 (2002);
- [10] O. Hess, Ch. Goddard, and S. Hess, *Physica A* **366**, 31 (2006)
- [11] R.G. Larson, *The Structure and Rheology of Complex Fluids*, Oxford University Press, Oxford, UK (1999).
- [12] S. Hess, *Z. Naturforsch.* **31a**, 1034 (1976).
- [13] A. Peterlin and H. A. Stuart, *Hand- und Jahrbuch der Chemischen Physik*, Vol. 8, p. 113, Ed. Eucken-Wolf (1943).
- [14] C. Zannoni, *Liquid crystal observables: static and dynamic properties*, in *Advances in the computer simulations of liquid crystals*, P. Pasini and C. Zannoni, eds., Kluwer Academic Publisher, Dordrecht (2000).
- [15] W. Muschik, H. Ehrentraut, and C. Papenfuss, *J. Non-Equilib. Thermodyn.* **22**, 285 (1997); W. Muschik and B. Su, *J. Chem. Phys.* **107**, 580 (1997).
- [16] G. G. Fuller, *Optical Rheometry of Complex Fluids* Oxford University Press, New York, 1995.
- [17] S. Heidenreich, P. Ilg, S. Hess, *Phys. Rev. E* **73**, 061710 (2006).
- [18] S. Hess, *Flow alignment of a colloidal solution which can undergo a transition from the isotropic to the nematic phase (Liquid crystal)*, in: *Electro-optics and dielectrics of macromolecules and colloids*, ed. B.R. Jennings, Plenum Publ. Corp. New York (1979).
- [19] M. Doi, *Ferroelectrics* **30**, 247 (1980); *J. Polym. Sci. Polym. Phys. Ed.* **19**, 229 (1981).
- [20] M. Grosso, R. Keunings, S. Crescitelli, and P.L. Maffettone, *Phys. Rev. Lett.* **86**, 3184 (2001).
- [21] M. G. Forest, R. Zhou, and Q. Wang, *J. Rheol.* **47**, 105 (2003);
- [22] J. L. Ericksen, *Trans. Soc. Rheol.* **5**, 23 (1961); F.M. Leslie, *Arch. Ration. Mech. Anal.* **28**, 265 (1968).
- [23] P. G. de Gennes, *The Physics of Liquid Crystals* (Clarendon Press, Oxford, 1974); H. Kelker and R. Hatz, *Handbook of Liquid Crystals* (Verlag Chemie, Weinheim, Deerfield, 1980).
- [24] G. B. Jeffrey, *Proc. R. Soc. London Ser. A* **102**, 171 (1922).
- [25] J. Feng, C. V. Chaubal, and L. G. Leal, *J. Rheol.* **42**, 1095 (1998).

- [26] P. Kaiser, W. Wiese, and S. Hess, *J. Non-Equilib. Thermodyn.* **17**, 153 (1992).
- [27] P. D. Olmsted and P. Goldbart, *Phys. Rev. A* **41**, 4578 (1990); *Phys. Rev. A* **46**, 4966 (1992); H. See, M. Doi, and R. Larson, *J. Chem. Phys.* **92**, 792 (1990).
- [28] V. Schmitt, F. Lequeux, A. Pousse, and D. Roux, *Langmuir* **10**, 955 (1994); A. S. Wunenburger, A. Colin, J. Leng, A. Arnedeo, and D. Roux, *Phys. Rev. Lett.* **86**, 1374 (2001); J.F. Berret, D.C. Roux, G. Porte, and P. Lindner, *Europhys. Lett.* **25**, 521 (2002).
- [29] C. Pujolle-Robic, P.D. Olmsted and L. Noirez, *Europhys.Lett.* **59**, 364 (2002).
- [30] S. Hess and P. Ilg, *Rheol.Acta*, **44**, 465 (2005); P. Ilg and S. Hess, *JNNFM* (2006).
- [31] N. Herdegen and S. Hess, *Physica A* **115** (1982) 281.
- [32] W. Loose and S. Hess, *Phys. Rev. Lett.* **58** (1988) 2443; *Phys. Rev. A* **37** (1988) 2099.
- [33] S. Hess, *Physica A* **118**, 79 (1983).
- [34] D. Severin, Inst.f.Maschinenkonstruktion, TU Berlin, private communication.
- [35] M.E. Cates, D.A. Head, and A. Ajdari, *Phys. Rev. E* **66**, 025202 (2002).
- [36] D.J. Evans and D.J. Searls, *Adv.in Phys.* **51**, 1529 (2002); G.M. Wang, E.M. Sevick, E. Mittag, D.J. Searls, and D.J. Evans, *Phys.Rev.Lett.* **89** 050601 (2002).
- [37] S. Hess and M. Kröger, *Phys.Rev. E* **64**, 011201 (2001)
- [38] M. Ellero, M. Kröger, and S. Hess: *J. Non-Newtonian Fluid Mech.* **105**, 35 (2002).

[a] Siegfried Hess, Sebastian Heidenreich, Patrick Ilg
Technische Universität Berlin, PN 7-1
Institut für Theoretische Physik
Hardenbergstr. 36
D-10623 Berlin, Germany
* **E-mail:** S.Hess@physik.tu-berlin.de

[b] Chris Goddard, Ortwin Hess
University of Surrey
Advanced Technological Institute
School of Electronics and Physical Sciences
Gu2 7XH, UK